Charge distributions for the photofission of ^{235}U and ^{238}U with 12—30 MeV bremsstrahlung

D. De Frenne, H. Thierens, B. Proot, E. Jacobs, P. De Gelder, and A. De Clercq
Nuclear Physics Laboratory, B-9000 Gent, Belgium

W. Westmeier
Kernchemie, Phillipps-Universität, D-3550 Marburg, West Germany
(Received 7 May 1982)

A systematic study of the charge distribution for bremsstrahlung-induced photofission of ^{235}U and ^{238}U with the end point energies ranging from 12 to 30 MeV was performed using direct γ-ray spectrometry of irradiated uranium samples or of fission product catcherfoils, and also employing chemical separation techniques. For both fissioning systems the width of the charge distribution was found to be practically independent of the average excitation energy and the values obtained are in very good agreement with those reported in the literature for low-energy fission. The deviation of the most probable charge Z_p from the unchanged charge density value Z_{UCD} as a function of the fragment mass shows the influence of the 50-proton shell in the charge distributions and a higher charge-to-mass ratio of the light fragments independent of the compound nucleus excitation energy. For the necessary conversion of postneutron into preneutron masses, neutron emission curves, $v(m^*)$, were deduced from previously measured postneutron and provisional mass distributions. Calculations following the scission-point model of Wilkins et al. and the predictions of the empirical relation of Nethaway reproduce very well the experimentally determined Z_p behavior, except in the mass region affected by the $Z=50$ closed shell.

NUCLEAR REACTIONS, FISSION ^{235,238}U(γ,F), $E_{\gamma max}=12$, 15, 20, 30 MeV; measured product γ-ray spectra; deduced charge distributions, width, and most probable charges; calculated $v(m^*)$ from measured provisional and postneutron mass distributions.

I. INTRODUCTION

New information on the nuclear charge distribution in low energy fission has appeared recently.[1−3] The dependence of the charge distribution on fragment kinetic energy was investigated using energy loss techniques[1,2] for the light-wing fission products and radiochemical measurements after mass and velocity preselection for the heavy-region fission products.[3] These studies revealed that the enhanced production of even-Z fragments persists over the whole investigated kinetic energy range, indicating that the internal excitation energy is tied up almost entirely in the collective degrees of freedom and that low energy fission is a weakly dissipative process. A comparative radiochemical investigation of the thermal and 3 MeV neutron induced fission of ^{235}U (Ref. 1) has shown that the odd-even effects on the charge yields, which amount to $22\pm7\%$ in

^{235}U(n_{th},f), are almost completely washed out ($5\pm3\%$) by an increase of the fissioning nucleus excitation energy by 3 MeV, probably due to quasiparticle excitations at the saddle point. Another very important conclusion of Lang et al.[2] from their study of ^{235}U(n_{th},f) was the independence of the width of the preneutron charge distribution from the total fragment excitation energy. According to these authors the value 0.40 ± 0.05 for the variance σ_Z^2 of the charge distribution may be an indication for quantum mechanical zero point oscillations, as statistical models and models based on the assumption of a quasiequilibrium of the collective degrees of freedom at the scission point predict smaller values for σ_Z^2. In the charge distribution summed over the kinetic energy, neglecting oscillations due to the proton odd-even effect, the deviation of the average charge $\bar{Z}$ from the unchanged charge density value Z_{UCD} as a function of the fragment mass

was found to remain constant at 0.6 charge units, except in the vicinity of the closed 50 proton shell, where $\bar{Z}$ follows the $Z = 50$ line.[2]

In contrast to low energy fission there are no new data on the behavior of the charge distribution in medium energy fission reported in the literature recently, so the information on the shape of the charge distribution in the considered excitation energy range remains very scarce. From a radiochemical determination of the independent yields of a number of long-lived fission products in the fission of ^{232}Th with protons of energies between 8 and 87 MeV, Pate et al.[4] deduced that the full width at half maximum of the charge distribution has a constant value of 2.2 charge units up to 25 MeV and increases at higher bombarding energies. However, the corresponding value for the variance σ_Z^2 is about twice the value measured directly in low energy fission with the present techniques. A systematic study of the excitation functions of the Cs isotopes in the proton induced fission of several heavy elements led Yaffe[5] to the conclusion that the charge distribution broadens with increasing excitation energy in the energy range between 20 and 85 MeV. McHugh and Michel[6] found that independent yields of the isobaric chain with mass 135 in the α-induced fission of ^{232}Th in the excitation energy range between 15 and 39 MeV can be represented by a Gaussian with a constant value of 0.95 ± 0.05 for the width parameter $c \simeq 2(\sigma_Z^2 + \frac{1}{12})$, which is very close to the ^{235}U(n_{th}, f) value 0.80 ± 0.14 (Ref. 7) deduced from radiochemical measurements. These data would suggest that the width of the charge distribution is varying only very slowly with the compound nucleus excitation energy up to 39 MeV. This trend is also supported by the average value 0.57 ± 0.04 for the charge distribution width σ_Z (corresponding to a c value of 0.82 ± 0.08), derived by Bocquet et al.[8] from yield measurements of noble-gas isotopes in the 14 MeV neutron induced fission of ^{233,235,238}U and ^{232}Th, and the average value 0.93 ± 0.06 reported for the width parameter c in our previous paper[9] on the photofission of ^{238}U with 20 MeV bremsstrahlung.

In this paper we present the results of an extensive study of the charge distribution for the photofission of ^{235}U and ^{238}U as a function of the end point energy of the bremsstrahlung in the energy range between 12 and 30 MeV. The independent and cumulative yields of short-lived ($5 \text{ s} < T_{1/2} < 20$ min) fission products were determined by direct γ-ray spectrometry of irradiated uranium samples. In addition to γ-ray spectrometry of fission product

catcher foils, chemical separation techniques were used for the determination of the independent yields of long-lived fission products. Thus it was possible to measure the fractional independent and cumulative chain yields of 50 fission products for the photofission of ^{235}U and 51 for ^{238}U. Using this set of data the width parameter c of the charge distribution was deduced for eight isobaric chains for ^{235}U and six for ^{238}U photofission. The average c values obtained are in very good agreement with those found in low-energy fission and show a tendency to increase slightly with the bremsstrahlung end point energy, attributable to an enhanced neutron emission. Furthermore, values for the most probable charge Z_p are deduced for 25 mass chains in the photofission of ^{235}U and 24 for ^{238}U. The deviation of Z_p from the unchanged charge density value Z_{UCD} shows the influence of the 50 proton shell and a charge polarization, resulting in a higher charge-to-mass ratio of the light fragment, independent of the compound nucleus excitation energy. The neutron emission curve, necessary for the conversion of the postneutron into preneutron masses, was deduced from the measured provisional and postneutron mass distribution. The experimentally determined Z_p values are compared to the expectations of Nethaway.[10] The results are discussed in the framework of the scission-point model of Wilkins et al.[11]

II. EXPERIMENTAL PROCEDURE

Information on the experimental setup and the procedure used for the determination of the independent yields of long-lived fission products via γ-ray spectrometry of fission product catcher foils can be found in previous papers.[12,13] To obtain the independent yields of ^{96}Nb, ^{124}Sb^g, ^{126}Sb^g, ^{126}Sb^m, ^{132}I^g, ^{132}I^m, ^{134}I^g, ^{134}I^m, ^{134}Cs, and ^{136}Cs for ^{238}U(γ, F), chemical separations on samples containing 1 g UO$_2$(NO$_3$)$_2 \cdot$6H$_2$O (natural uranium), irradiated for appropriate times, were performed. The procedures used for the separation of the niobium, antimony, iodine, and cesium fractions were adopted from Morris et al.,[14] Dropesky and Orth,[15] Troutner et al.,[16] and Cuninghame et al.,[17] respectively. As fission yield monitors we used ^{97}Nb, ^{127}Sb, ^{131}Sb, ^{135}I, and ^{137}Cs. For the determination of the independent yields of ^{130}I^{g+m}, ^{132}I^{g+m}, ^{133}I, ^{134}I^g, and ^{134}I^m in ^{235}U(γ, F) the iodine fraction was chemically separated from fission product catcher foils.

Successive γ-ray spectra of the separated samples were taken using a 50 cm^3 Ortec Ge(Li) detector and conventional electronics. The resolution of the system was 1.8 keV FWHM at 1333 keV.

As mentioned in the Introduction the fractional independent and cumulative yields of short-lived fission products with half-lives as short as 5 s were determined by direct γ-ray spectrometry of irradiated uranium samples. For our ^{238}U(γ,F) study we used 0.1 mm thick natural uranium metallic disks; in the case of ^{235}U(γ,F) the samples were 0.2 mm thick and enriched up to 97% in ^{235}U. The uranium disks, prepared at the Central Bureau for Nuclear Measurements (Euratom, Geel), were enclosed in pure nickel capsules (99.99%). After an irradiation for 30 s with a 12, 15, 20, or 30 MeV bremsstrahlung beam produced in a 0.1 mm thick Au converter, the capsules were transported from the irradiation site to the Ge(Li) detector with a pneumatic transport system. Starting 5 s after the end of the irradiation, 60 consecutive γ-ray spectra with a measuring time of 10 s each were taken, using the same Ge(Li) detector and measuring setup as used for the determination of the yields of longer-lived fission products after chemical separation. The 60 spectra were recorded as one single file on an RK05 disk with a PDP 11/10 system and a CA11C CAMAC interface. The time interval between two successive spectra was less than 150 μs. More information on the program can be found in Ref. 18. The variation of the dead time during the measur-

ing cycle was followed with the pulser technique. Several successive spectra, chosen according to the half-life of the fission product considered in the analysis, were added up later. The identification of the γ rays in the spectra was mainly based on the γ-ray catalogs of Reus *et al.*[19] and Blachot and Fiche.[20] The decay data which are used for the calculation of the fission yields but not tabulated in previous papers (Refs. 9, 12, 13, 21, and 22) are summarized in Table I. The fission product nuclide, the energy (E_γ), the absolute intensity (I_γ) of the observed γ transition, the half-lives of the nuclide $(T_{1/2})$ and its precursor $(T_{1/2p})$, and the reference from which the data were adopted are given in the table. The absolute intensity of the 504.3 keV γ ray in the decay of ^{100}Zr was deduced from the absolute intensity of the 535.2 keV γ ray in the decay of the daughter ^{100}Nb^A $(T_{1/2}=1.5$ s), 50.0%, given in Ref. 20.

The peak areas in the γ spectra were calculated with the programs MARKER and CAOS of Westmeier.[32] The half-life of the peaks used in the calculations was carefully checked and the corresponding fractional independent or cumulative yields were calculated using a modified version of the fitting program CLSQ of Cumming.[33] In this version successive β decay is taken into account. As mentioned in a previous paper,[13] the contribution of slow neutron induced fission in the photofission experiments on ^{235}U was determined by replacing the uranium target by scandium and indium samples.

TABLE I. Nuclear data for fission products.

Nuclide	E_γ (keV)	I_γ (%)	$T_{1/2}$	$T_{1/2p}$	Reference
^{89}Kr	585.8	18.6	3.07 min	4.53 s	23
^{96}Nb	778.2	96.9	23.4 h		24
^{100}Zr	504.3	34.8^a	7.1 s	0.55 s, 0.94 s	25
^{124}Sb^g	602.7	98.4	60.2 d	20.2 min, 93 s	26
	1691.0	49.0			
^{129}Sn^A	645.1	98.5	2.4 min	1.29 s, 0.59 s	27
^{129}Sn^B	1128.45	45.8	6.9 min	1.29 s, 0.59 s	27
	1161.3	52.6			
^{130}Sn^g	779.8	59.1	223 s	0.53 s, 0.53 s, 0.33 s	28, 29
^{130}Sb^A	1017.5	30.0	6.3 min	223 s	29
^{130}Sb^B	839.4	100	40 min	1.7 min	29
	793.4	100			
^{134}Sb	297	97	11 s	1.04 s	3
	1279	100			
^{141}Cs	561	5.8	24.94 s	1.72 s	30
^{142}Ba	1000.9	13.18	10.7 min	1.7 s	20
^{143}Ba	798.0	16	14.5 s	1.78 s	31

$^a I_\gamma$ value obtained in this work.

For 30 MeV bremsstrahlung an upper limit of 2% was obtained.

III. RESULTS AND DISCUSSION

The fractional independent and cumulative chain yields for the photofission of ^{235}U and ^{238}U with 12-, 15-, 20-, and 30-MeV bremsstrahlung, obtained in this work, are summarized in Tables II and III. The uncertainties indicated in the tables are calculated as outlined in Ref. 21. A determination of the independent yields of the 21 min ^{124}Sb^m(8$^-$), 93 s ^{124}Sb^m(5$^+$), 1.7 min ^{130}Sn^m(7$^-$), 9.0 min ^{130}I^m(2$^+$), and 0.85 s ^{134}Sb(LS) isomers was impossible in the performed experiments. The fraction of the total yield of ^{124}Sb (18%) not decaying via the ground state was adopted from ^{235}U(n_{th},f) data[34] and for ^{130}I (14%) from the proton induced fission of ^{238}U (Ref. 35). The contribution of the ^{130}Sn(7$^-$) and ^{134}Sb(LS) isomers in the total yield of ^{130}Sn and ^{134}Sb was calculated by assuming, for the isomeric ratios,

$$\frac{^{130}\text{Sn}(7^-)}{^{130}\text{Sn}(0^+)}$$

and

$$\frac{^{134}\text{Sb}(LS)}{^{134}\text{Sb}(HS)},$$

the same values in ^{235}U(γ,F) and ^{238}U(γ,F) as in ^{235}U(n_{th},f), namely 0.09 (Ref. 31) and 0.20 (Ref. 36), respectively. This procedure for the estimation of the yields of these isomers is supported by the close agreement between the values for the isomeric ratios reported in the literature for ^{235}U(n_{th},f) and

those determined in our earlier photofission work.[12,13] The corrections for the isomer yields are already included in Tables II and III.

In these tables the total fractional cumulative yield of ^{131}Sn is given but the yields of ^{131}Sn^m and ^{131}Sn^g are not mentioned separately, owing to the incompleteness of the β-decay scheme of these isomers. In a recent paper[37] the most intense β branches in the decay of ^{131}Sn^m and ^{131}Sn^g to levels in ^{131}Sb are reported, showing that ^{131}Sn^m and ^{131}Sn^g are decaying to the ^{131}Sb ground state mainly via the 1226.6 and 798.4 keV γ rays, respectively. However, the assignment of a number of weak γ transitions to the ground state of ^{131}Sb remains doubtful, introducing serious uncertainties on the absolute intensities of the 798.4 and 1226.6 keV γ rays. Two extreme cases were considered for the calculation of absolute intensities of these γ rays: assignment of the unidentified γ transitions to the ground state of ^{131}Sb to the decay of ^{131}Sn^m yields $I_{798.4}=0.73$, $I_{1226.2}=0.68$, and assignment to the decay of ^{131}Sn^g yields $I_{798.4}=0.52$, $I_{1226.2}=1.0$. Although the corresponding yield of the isomers differs significantly, the total yield of ^{131}Sn remains the same within 5%. In Tables II and III the average values for the fractional cumulative yields of ^{131}Sn, obtained in the two considered cases, are given and the uncertainties, resulting from the adopted procedure, are included in the errors.

As pointed out in a previous paper,[9] based on the assumption of a Gaussian shape for the charge distribution in fission induced by monoenergetic photons with energy k, the charge distribution in our bremsstrahlung experiments $P(Z)$ can be represented by the following expression:

$$P(Z)=\frac{\int_0^{E_e} \frac{1}{\sqrt{\pi c}}\exp\left[-\frac{[Z-Z_p(k)]^2}{c}\sigma_{\gamma,F}(k)\phi(E_e,k)dk\right]}{\int_0^{E_e}\sigma_{\gamma,F}(k)\phi(E_e,k)dk}. \tag{1}$$

For the bremsstrahlung spectrum with an end point energy $E_e,\phi(E_e,k)$ we used the Schiff form.[38] The photofission cross sections $\sigma_{\gamma,F}(k)$ for ^{235}U and ^{238}U up to 18 MeV were adopted from Caldwell et al.[39] As indicated in Refs. 12 and 13 an estimate of the cross section above 18 MeV was obtained by an extrapolation procedure, proposed by Shotter et al.[40] The shift of the maximum of the charge distribution $Z_p(k)$ with the photon energy k was taken from the study of Nethaway.[10] The width parameter c of the charge distribution in expression (1) was assumed to be independent of the photon en-

ergy k. The assumption of the constancy of c in the considered excitation energy range is supported by the results, obtained in particle induced fission, as mentioned in the Introduction. The existence of odd-even effects on the charge distribution was not taken into account in expression (1). Following Mariolopoulos et al.[1] a crude calculation of the number of proton pair breakings at the saddle point was performed and the probability for pair breaking from the saddle to the scission point was adopted from ^{235}U(n_{th},f) as 0.78. These calculations yield estimated values of 5% and 3% for the odd-even

TABLE II. Fractional independent and cumulative chain yields for the photofission of ^{235}U. (c) denotes the fractional cumulative chain yield.

Nuclide \ E_e (MeV)	12	15	20	30
^{88}Br(c)	0.434±0.042	0.427±0.042	0.396±0.035	0.408±0.040
^{89}Kr(c)	0.870±0.084	0.842±0.079	0.852±0.079	0.867±0.084
^{90}Kr(c)	0.595±0.076	0.628±0.079	0.599±0.075	0.602±0.076
^{91}Kr(c)	0.372±0.037	0.377±0.124	0.342±0.035	0.304±0.033
^{93}Rb(c)	0.441±0.089	0.482±0.066	0.419±0.103	
^{94}Sr(c)	0.802±0.099	0.817±0.088	0.762±0.080	0.787±0.083
^{95}Sr(c)	0.641±0.063	0.634±0.056	0.579±0.053	0.625±0.058
^{100}Zr(c)	0.704±0.091	0.677±0.102	0.604±0.076	0.598±0.108
^{126}Sb^g		$(5.9\ \pm2.2)\times10^{-2}$	$(8.2\ \pm1.7)\times10^{-2}$	0.110±0.017
^{126}Sb^m		$(6.4\ \pm2.0)\times10^{-2}$	$(6.7\ \pm1.7)\times10^{-2}$	$(8.0\ \pm1.9)\times10^{-2}$
^{128}Sn(c)		0.685±0.053	0.661±0.046	0.611±0.049
^{129}Sb$^A(\frac{11}{2}^-)$(c)	0.253±0.020	0.196±0.012	0.186±0.013	0.180±0.016
^{129}Sb$^B(\frac{3}{2}^+)$(c)	0.151±0.011	0.146±0.009	0.133±0.009	0.123±0.009
^{130}Sn(c)	0.258±0.020	0.236±0.019	0.241±0.034	0.173±0.020
^{130}Sb$^A(5^+)$	0.293±0.137	0.248±0.072	0.220±0.059	0.250±0.063
^{130}Sb$^B(8^-)$	0.331±0.030	0.281±0.020	0.296±0.016	0.275±0.011
^{130}I		$(3.6\ \pm1.7)\times10^{-3}$	$(5.7\ \pm1.0)\times10^{-3}$	$(9.8\ \pm1.6)\times10^{-3}$
^{131}Sn(c)	0.119±0.010	0.110±0.006	0.114±0.007	0.122±0.007
^{131}Sb	0.549±0.066	0.485±0.045	0.416±0.047	0.410±0.040
^{131}Te^g	0.125±0.052	0.151±0.034	0.167±0.028	0.168±0.037
^{131}Te^m	0.180±0.023	0.215±0.019	0.263±0.026	0.270±0.023
^{132}Sn	$(3.2\ \pm1.8)\times10^{-2}$	$(2.2\ \pm0.7)\times10^{-2}$	$(2.5\ \pm0.7)\times10^{-2}$	$(3.0\ \pm0.8)\times10^{-2}$
^{132}Sb^g	0.138±0.017	0.100±0.010	$(7.5\ \pm0.9)\times10^{-2}$	$(9.8\ \pm1.3)\times10^{-2}$
^{132}Sb^m	0.202±0.054	0.214±0.023	0.187±0.020	0.192±0.022
^{132}Te	0.562±0.094	0.602±0.052	0.629±0.065	0.592±0.028
^{132}I	$(4.6\ \pm1.9)\times10^{-2}$	$(6.2\ \pm0.6)\times10^{-2}$	$(7.6\ \pm0.8)\times10^{-2}$	$(9.1\ \pm0.9)\times10^{-2}$
^{133}Sb	0.196±0.019	0.175±0.017	0.162±0.013	0.179±0.018
^{133}Te^g	0.203±0.043	0.214±0.032	0.175±0.072	0.167±0.038
^{133}Te^m	0.473±0.062	0.471±0.040	0.454±0.042	0.404±0.041
^{133}I	0.118±0.042	0.153±0.034	0.180±0.025	0.181±0.035
^{134}Sb	$(3.6\ \pm0.6)\times10^{-2}$	$(3.0\ \pm0.2)\times10^{-2}$	$(2.3\ \pm0.4)\times10^{-2}$	$(2.3\ \pm0.4)\times10^{-2}$
^{134}Te	0.52±0.05	0.51±0.05	0.48±0.05	0.53±0.10
^{134}I	0.36±0.07	0.40±0.06	0.40±0.05	0.42±0.08
^{135}Te	0.237±0.006	0.171±0.035	0.147±0.031	0.203±0.040
^{135}I	0.603±0.083	0.623±0.056	0.625±0.050	0.562±0.052
^{135}Xe	0.160±0.021	0.206±0.017	0.228±0.016	0.245±0.012
^{136}Te	$(6.4\ \pm0.5)\times10^{-2}$	$(5.7\ \pm0.9)\times10^{-2}$	$(5.3\ \pm0.7)\times10^{-2}$	$(7.0\ \pm0.4)\times10^{-2}$
^{136}I^g	$(8.9\ \pm1.4)\times10^{-2}$	$(7.1\ \pm2.3)\times10^{-2}$	$(7.7\ \pm1.3)\times10^{-2}$	$(8.3\ \pm1.2)\times10^{-2}$
^{136}I^m	0.212±0.018	0.225±0.014	0.199±0.017	0.207±0.017
^{136}Cs		$(2.0\ \pm0.5)\times10^{-2}$	$(2.9\ \pm0.5)\times10^{-2}$	$(3.6\ \pm0.5)\times10^{-2}$
^{137}I(c)	0.334±0.045	0.326±0.075	0.294±0.069	0.364±0.068
^{137}Xe	0.567±0.114	0.548±0.070	0.483±0.087	0.455±0.078
^{138}Xe(c)	0.725±0.115	0.679±0.079	0.589±0.091	0.613±0.093
^{138}Cs	0.250±0.070	0.350±0.078	0.360±0.062	0.390±0.071
^{139}Xe(c)	0.547±0.074	0.447±0.065	0.380±0.048	0.418±0.053
^{140}Xe(c)	0.248±0.025	0.245±0.025	0.218±0.018	0.223±0.019
^{140}Cs	0.583±0.098	0.576±0.063	0.538±0.081	0.524±0.085
^{141}Cs(c)	0.611±0.040	0.643±0.056	0.610±0.082	0.629±0.070
^{142}Ba(c)		0.894±0.096	0.866±0.053	0.846±0.091
^{143}Ba(c)	0.775±0.105	0.782±0.061	0.685±0.060	0.666±0.055

TABLE III. Fractional independent and cumulative chain yields for the photofission of ^{238}U. (c) denotes the fractional cumulative chain yield.

Nuclide \ E_e (MeV)	12	15	20	30
^{88}Br(c)	0.810 ± 0.085	0.788 ± 0.073	0.740 ± 0.080	0.788 ± 0.078
^{90}Kr(c)	0.853 ± 0.107	0.803 ± 0.101	0.838 ± 0.093	0.772 ± 0.098
^{91}Kr(c)	0.725 ± 0.107	0.655 ± 0.063	0.665 ± 0.087	0.683 ± 0.133
^{93}Rb(c)	0.862 ± 0.190	0.625 ± 0.162	0.736 ± 0.130	
^{94}Sr(c)	0.870 ± 0.090	0.864 ± 0.083	0.884 ± 0.099	0.797 ± 0.084
^{95}Sr(c)	0.881 ± 0.078	0.823 ± 0.080	0.848 ± 0.071	0.875 ± 0.092
^{96}Nb		$(7.3\ \pm2.5)\times10^{-5}$	$(1.1\ \pm0.5)\times10^{-4}$	$(2.4\ \pm0.6)\times10^{-4}$
^{100}Zr(c)	0.915 ± 0.116	0.915 ± 0.116	0.870 ± 0.108	0.920 ± 0.115
^{124}Sb		$(1.36\ \pm0.63)\times10^{-3}$	$(2.07\ \pm0.36)\times10^{-3}$	$(3.98\ \pm0.59)\times10^{-3}$
^{126}Sb^g	$(1.18\ \pm0.09)\times10^{-2}$	$(1.45\ \pm0.07)\times10^{-2}$	$(1.81\ \pm0.10)\times10^{-2}$	$(2.96\ \pm0.12)\times10^{-2}$
^{126}Sb^m		$(1.07\ \pm0.24)\times10^{-2}$	$(1.30\ \pm0.32)\times10^{-2}$	$(1.78\ \pm0.24)\times10^{-2}$
^{128}Sn(c)	0.770 ± 0.120	0.670 ± 0.110	0.700 ± 0.090	0.702 ± 0.090
^{128}Sb^g		$(4.9\ \pm1.9)\times10^{-2}$	$(6.2\ \pm2.3)\times10^{-2}$	$(8.5\ \pm2.4)\times10^{-2}$
^{129}Sn$^A(\frac{11}{2}^-)(c)$	0.475 ± 0.056	0.363 ± 0.044	0.297 ± 0.036	0.304 ± 0.036
^{129}Sn$^B(\frac{3}{2}^+)(c)$	0.316 ± 0.043	0.263 ± 0.034	0.277 ± 0.033	0.250 ± 0.030
^{130}Sn(c)	0.453 ± 0.036	0.410 ± 0.031	0.400 ± 0.046	0.380 ± 0.040
^{130}Sb$^A(5^+)$	$0.20\ \pm0.10$	$0.14\ \pm0.07$	$0.17\ \pm0.10$	$0.18\ \pm0.11$
^{130}Sb$^B(8^-)$	0.292 ± 0.034	0.229 ± 0.023	0.296 ± 0.017	0.329 ± 0.014
^{131}Sn(c)	0.380 ± 0.035	0.349 ± 0.028	0.334 ± 0.050	0.341 ± 0.021
^{131}Sb	0.507 ± 0.075	0.506 ± 0.054	0.494 ± 0.058	0.457 ± 0.054
^{131}Te^g		$(7.8\ \pm4.8)\times10^{-2}$	$(8.5\ \pm4.5)\times10^{-2}$	$(9.3\ \pm4.3)\times10^{-2}$
^{131}Te^m	$(2.9\ \pm0.7)\times10^{-2}$	$(5.7\ \pm1.1)\times10^{-2}$	$(7.7\ \pm1.1)\times10^{-2}$	0.100 ± 0.013
^{132}Sn	0.249 ± 0.021	0.222 ± 0.017	0.181 ± 0.019	0.182 ± 0.017
^{132}Sb^g	0.186 ± 0.049	0.202 ± 0.023	0.169 ± 0.037	0.217 ± 0.033
^{132}Sb^m	0.328 ± 0.055	0.312 ± 0.075	0.339 ± 0.051	0.317 ± 0.118
^{132}Te	$0.24\ \pm0.12$	$0.25\ \pm0.11$	$0.31\ \pm0.10$	$0.28\ \pm0.17$
^{132}I^g		$(5.7\ \pm1.4)\times10^{-3}$	$(7.4\ \pm1.5)\times10^{-3}$	$(1.17\ \pm0.21)\times10^{-2}$
^{132}I^m		$(3.9\ \pm1.2)\times10^{-3}$	$(5.7\ \pm0.9)\times10^{-3}$	$(1.26\ \pm0.17)\times10^{-2}$
^{133}Sb(c)	0.487 ± 0.032	0.498 ± 0.032	0.450 ± 0.046	0.492 ± 0.054
^{133}Te^g	0.173 ± 0.031	0.156 ± 0.041	0.147 ± 0.040	0.135 ± 0.039
^{133}Te^m	0.302 ± 0.026	0.267 ± 0.035	0.348 ± 0.034	0.277 ± 0.034
^{133}I	$(3.5\ \pm2.0)\times10^{-2}$	$(7.4\ \pm2.1)\times10^{-2}$	$(9.5\ \pm2.6)\times10^{-2}$	0.101 ± 0.031
^{134}Sb	0.136 ± 0.008	0.102 ± 0.006	0.102 ± 0.006	$(9.3\ \pm0.7)\times10^{-2}$
^{134}Te	0.695 ± 0.012	0.685 ± 0.030	0.671 ± 0.034	0.665 ± 0.030
^{134}I	0.169 ± 0.041	0.213 ± 0.024	0.227 ± 0.028	0.255 ± 0.023
^{134}Cs			$(4.0\ \pm1.5)\times10^{-5}$	$(8.6\ \pm3.4)\times10^{-5}$
^{135}Te(c)	0.532 ± 0.113	0.530 ± 0.088	0.567 ± 0.060	0.538 ± 0.090
^{135}I	0.433 ± 0.128	0.426 ± 0.105	0.393 ± 0.078	0.402 ± 0.102
^{135}Xe	0.035 ± 0.015	0.044 ± 0.017	0.051 ± 0.012	0.060 ± 0.012
^{136}Te	0.285 ± 0.017	0.228 ± 0.018	0.230 ± 0.028	0.167 ± 0.026
^{136}I^g	0.113 ± 0.044	0.138 ± 0.044	0.109 ± 0.017	0.144 ± 0.056
^{136}I^m	0.269 ± 0.015	0.256 ± 0.015	0.304 ± 0.039	0.364 ± 0.051
^{136}Cs	$(4.6\ \pm1.1)\times10^{-4}$	$(1.06\ \pm0.11)\times10^{-3}$	$(1.86\ \pm0.16)\times10^{-3}$	$(3.62\ \pm0.32)\times10^{-3}$
^{137}I(c)	0.713 ± 0.103	0.709 ± 0.063	0.679 ± 0.080	0.577 ± 0.072
^{137}Xe	0.249 ± 0.106	0.234 ± 0.051	0.266 ± 0.056	$0.42\ \pm0.18$
^{138}I(c)	0.311 ± 0.027	0.334 ± 0.048	0.300 ± 0.036	0.292 ± 0.034
^{139}Xe(c)	0.923 ± 0.107	0.812 ± 0.095	0.812 ± 0.084	
^{140}Xe(c)	0.686 ± 0.050	0.637 ± 0.051	0.594 ± 0.065	0.587 ± 0.059
^{140}Cs	0.314 ± 0.055	0.363 ± 0.056	0.416 ± 0.053	0.413 ± 0.064
^{144}Ba(c)	0.756 ± 0.068	0.789 ± 0.054	0.788 ± 0.084	0.790 ± 0.067
^{144}La	0.244 ± 0.067	0.244 ± 0.061	0.237 ± 0.078	0.210 ± 0.025

effects in our photofission experiments with 12 and 15 MeV bremsstrahlung, respectively. In view of the uncertainties on the measured yields, given in Tables II and III, the existence of odd-even effects can be neglected.

By a least-squares fit of the experimentally determined yields to expression (1), the width parameter c and the maximum of the charge distribution Z_p were deduced for the mass chains for which at least two fractional independent or cumulative yields were obtained. The c values resulting from this fitting procedure for the photofission of ^{235}U and ^{238}U are given in Tables IV and V, respectively. The average c values, for each bremsstrahlung end point energy $\langle c \rangle$, as well as the values for the average compound nucleus excitation energy adopted from Refs. 12 and 13, $\langle E_{exc} \rangle$, are also included in the tables. A survey of the results, summarized in Tables IV and V, shows that the values for the width of the charge distribution for mass 134 are significantly smaller than those for other mass chains in both fissioning systems throughout the whole considered excitation energy range. On the contrary, our photofission experiments yield rather high c values for mass 131, compared to the average, especially for 20 and 30 MeV bremsstrahlung. A very low value for the charge dispersion at mass 134 ($c=0.51$) was also reported in $^{235}U(n_{th},f)$ (Ref. 41), which was attributed to the abnormally high yield of the $N=82$ nucleus ^{134}Te. This also remains a plausible explanation for the low c value observed in our photofission work as the top of the charge distribution Z_p for mass 134 lies very close to $Z=52$ and a lowering of the ^{134}Te yield would result immediately in an increase of the charge distribution width for ^{235}U as well as for ^{238}U. Although a systematic higher $\langle c \rangle$ value for $A=131$ could

eventually be attributed to erroneous decay data, the observed increase of $\langle c \rangle$ with the bremsstrahlung end point energy is difficult to explain. This is perhaps related to the increased neutron emission in this mass region at higher excitation energies. The fractional independent yield of $^{136}I^{g+m}$, obtained in our experiments, is systematically about 33% lower than the expectation value, calculated from the fit of the ^{136}Te and ^{136}Cs data to expression (1), which yield the expected values of c and Z_p for mass 136. The c values, obtained by rejecting the $^{136}I^{g+m}$ data, are given in the tables. In their study of the charge distribution as a function of the kinetic energy of the fragments in $^{235}U(n_{th},f)$, Denschlag et al.[3] also reported very low yields of $^{136}I^{g+m}$ and consequently very high yields of the stable element ^{136}Xe, resulting in high values (1.40−1.63 according to the kinetic energy) for the odd-even factors. As such important nuclear structure effects on the yields at the average excitation energies, considered in our experiments, are very improbable and normal yields for the lighter iodine isotopes are obtained, the low yield of $^{136}I^{g+m}$ (Ref. 14) has to be due to incomplete information on the decay scheme of ^{136}I. A possible explanation for the overestimate of the absolute intensities of the γ rays in the decay of $^{136}I^{g+m}$ can be found in the fact that the β-decay energy of $^{136}I^{g}$ is high (7.0 ± 0.1 MeV), and that many final states in ^{136}Xe are available. This effect was shown by Hardy et al.[42] in their simulated study of the fictional nuclide pandemonium and illustrated by the same authors for the case of ^{145}Gd.

From Tables IV and V it is clear that, as well for the photofission of ^{235}U as for the photofission of ^{238}U, the average c value $\langle c \rangle$ increases slightly with the bremsstrahlung end point energy, although within the experimental uncertainties the constancy

TABLE IV. Values of the width parameter c determined for the photofission of ^{235}U. M_{post} denotes the postneutron mass.

M_{post} \ E_e (MeV)	12	15	20	30
130		0.86 ± 0.09	0.92 ± 0.06	0.90 ± 0.04
131	0.92 ± 0.14	1.02 ± 0.13	1.39 ± 0.18	1.45 ± 0.19
132	0.72 ± 0.12	0.71 ± 0.05	0.70 ± 0.05	0.76 ± 0.05
133	0.66 ± 0.10	0.68 ± 0.08	0.72 ± 0.08	0.79 ± 0.21
134	0.67 ± 0.07	0.63 ± 0.06	0.58 ± 0.06	0.55 ± 0.08
135	0.86 ± 0.14	0.82 ± 0.09	0.78 ± 0.09	1.00 ± 0.13
136		0.76 ± 0.05	0.79 ± 0.04	0.87 ± 0.03
140	0.92 ± 0.35	0.94 ± 0.23	1.09 ± 0.32	1.14 ± 0.35
$\langle c \rangle$	0.78 ± 0.12	0.80 ± 0.14	0.87 ± 0.24	0.93 ± 0.27
$\langle E_{exc} \rangle$ (MeV)	9.7	11.6	13.1	14.1

TABLE V. Values of the width parameter c determined for the photofission of ^{238}U. M_{post} denotes the postneutron mass.

M_{post} \ E_e (MeV)	12	15	20	30
131		1.09±0.22	1.19±0.27	1.43±0.32
132	1.23±0.29	0.97±0.06	0.94±0.05	1.05±0.05
133	0.75±0.16	1.12±0.21	1.03±0.19	1.31±0.32
134	0.65±0.02	0.63±0.03	0.69±0.05	0.64±0.32
135	0.82±0.22	0.90±0.23	1.06±0.21	1.06±0.04
136	0.67±0.02	0.68±0.02	0.73±0.03	0.70±0.04
$\langle c \rangle$	0.82±0.21	0.90±0.23	0.94±0.20	1.03±0.31
$\langle E_{exc} \rangle$ (MeV)	9.7	11.6	13.4	14.7

of $\langle c \rangle$ cannot be excluded. The values obtained for both fissioning systems are also nearly the same. The systematic slight increase of $\langle c \rangle$ with the bremsstrahlung end point energy can very probably be attributed to the enhanced neutron emission at high excitation energies. Previous studies[12,13] showed that the average number of emitted neutrons $\langle v \rangle$ increases from 2.78±0.12 to 3.25±0.14 for ^{235}U(γ,F) and from 2.85±0.11 to 3.57±0.11 for ^{238}U(γ,F) when the electron energy is raised from 12 to 30 MeV. The $\langle c \rangle$ values obtained in our photofission experiments are in good agreement with the value 0.80±0.14 given by Wahl et al.[7] for ^{235}U(n_{th},f), the value 0.82±0.08 derived by Bocquet et al.[8] for 14 MeV neutron induced fission of different actinides, and the c value 0.95±0.05 determined by McHugh and Michel[6] for mass 135 in the α-induced fission of ^{232}Th in the excitation energy range of 15−39 MeV. Our results confirm that the width of the charge distribution is nearly independent of the excitation energy of the fissioning nucleus up to about 15 MeV.

In the framework of the scission-point model of Wilkins et al.[11] in which a statistical equilibrium of the collective degrees of freedom at the scission point is assumed, the independence of c on the compound nucleus excitation energy indicates that the collective temperature, which is proportional to c, remains constant and that the additional excitation energy above the barrier goes into intrinsic excitations. However, based on the independence of c on the fragment excitation energy, Clerc et al.[43] showed that in the framework of semiequilibrium models the experimentally determined value for c corresponds to unrealistically high values for the collective excitation energy in view of the available total excitation energy of the fragments. It was also pointed out by Nifenecker et al.[44] that the propor-

tionality between the temperature T and the parameter c is very probably not valid since the condition $T \gg \hbar\omega/2$, with $\hbar\omega$ the phonon energy of the charge-to-mass ratio degree of freedom, is not fulfilled. The observed constancy of the width of the charge distribution with the excitation energy can then be understood in a thermodynamic equilibrium model if the quantum mechanical zero-point motion dominates over the temperature effects $T \ll \hbar\omega/2$ as proposed by Vandenbosch and Huizenga.[45]

For the mass chains for which the width parameter c was determined, the top of the distribution, the Z_p value, was calculated simultaneously. By adopting for c the average values $\langle c \rangle$, given in Tables IV and V, Z_p values were calculated using expression (1) for the mass chains for which the fractional independent or cumulative yield of only one member was determined. The deviations of the experimentally determined most probable charges Z_p from the charge of the fragments, calculated by assuming unchanged charge density of compound nucleus and fragments (Z_{UCD}), are plotted as a function of the preneutron emission mass m^* for the photofission of ^{235}U and ^{238}U in Figs. 1 and 2, respectively. The results for the light fragments are indicated by black squares, those for the heavy fragments by closed points.

For the conversion of the postneutron emission masses into preneutron emission masses, the neutron emission curve was calculated from previously published data on the provisional[46,47] and postneutron[12,13] mass distributions for the photofission of ^{235}U and ^{238}U, using an iterative procedure as described in Ref. 48. The values of the variance of the total number of emitted neutrons $\sigma^2(v)$ and the average variance $\langle \sigma^2(v,m) \rangle$ of the number of neutrons, emitted by the fragments with mass m, along
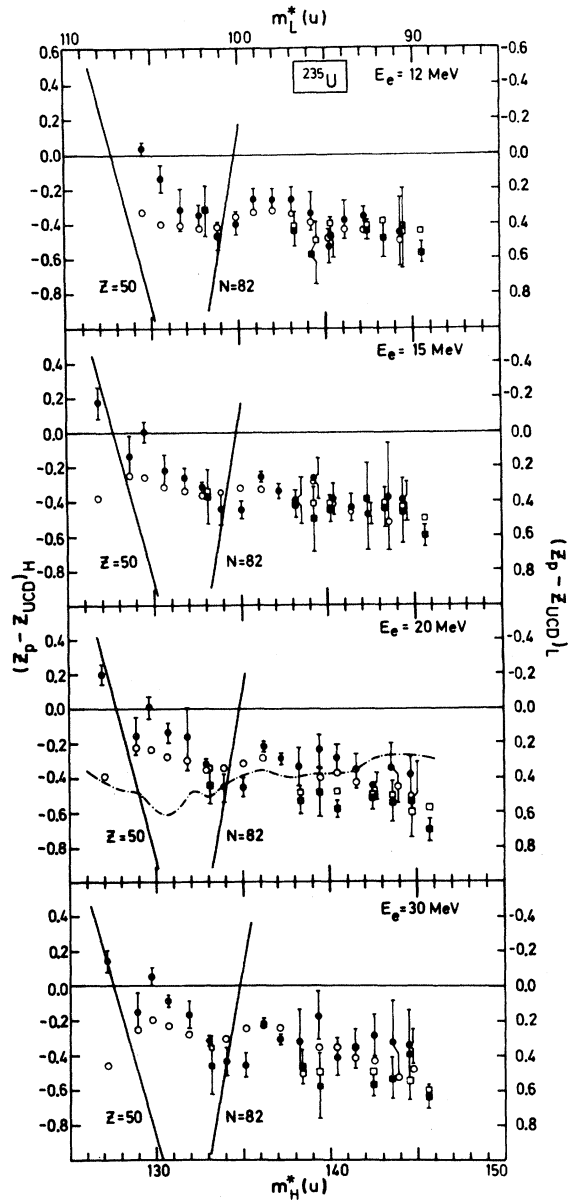
FIG. 1. Deviation of Z_p from Z_{UCD} as a function of the fragment mass m^* for the photofission of ^{235}U with 12-, 15-, 20-, and 30-MeV bremsstrahlung. Closed squares and points represent the experimentally determined Z_p values for the light and heavy fragments, respectively. The open symbols refer to the corresponding expectation values following Nethaway (Ref. 10). The dashed line in the 20-MeV section indicates the Z_p behavior, calculated with the scission-point model of Wilkins *et al.* (Ref. 11). The full lines correspond to the closed 50-proton and 82-neutron shells.

FIG. 2. Deviation of Z_p from Z_{UCD} as a function of the fragment mass m^* for the photofission of ^{238}U with 12-, 15-, 20-, and 30-MeV bremsstrahlung. The symbols have the same meaning as in Fig. 1.

with additional parameters which have to be known in these calculations, were adopted from ^{235}U(n_{th},f) (Ref. 49), as no information is available for photo-

fission. The values for the average center-of-mass energy of the neutrons η were deduced from the relation between η and the average total number of emitted neutrons $\langle v \rangle$, given by Caldwell *et al.*[39] for the photofission of different actinides.
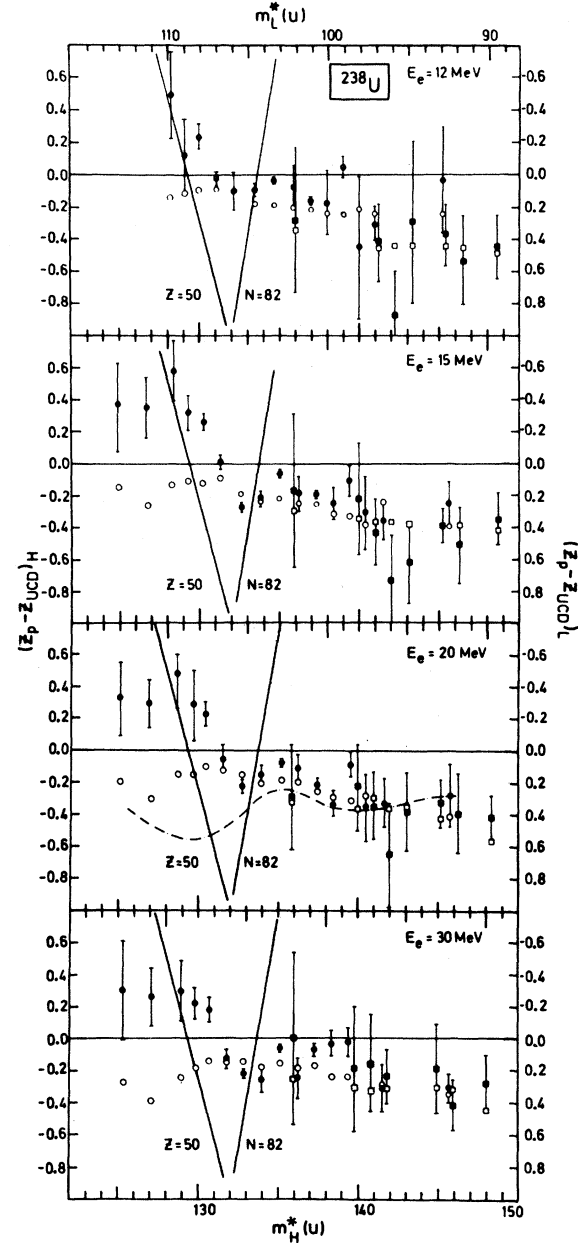
These neutron emission curves for the photofission of ^{235}U and ^{238}U with 12-, 15-, 20-, and 30-

MeV bremsstrahlung are depicted graphically in Figs. 3 and 4. From these figures it is apparent that the neutron emission curves show the typical sawtooth structure as usually observed in low energy fission (Ref. 45). As pointed out in Ref. 48, it is impossible to determine the neutron yields in the symmetric fission region with the iterative method used, owing to the divergence of the calculated errors. Estimated neutron yields in this region were determined by linear interpolation between the extreme points drawn in Figs. 3 and 4 around masses 110 and 130, for which an acceptable accuracy still can be obtained. They are represented by dashed lines in these figures. This procedure was based on the similarity of the $v(m^*)$ curves, obtained in this work for photofission and those measured for other low energy fissioning systems, especially for ^{235}U(n_{th}, f) (Refs. 50 and 51), where a maximum around mass 110 and a minimum around mass 129 are present and $v(m^*)$ decreases linearly in between.

A survey of Figs. 1 and 2 shows that the deviation of Z_p from the unchanged charge density value Z_{UCD} as a function of the fragment mass has a smooth behavior in both cases studied. The influence of the $Z=50$ shell on the charge distribution is also obvious from these figures, especially for the photofission of ^{238}U. This shell effect was also observed in ^{235}U(n_{th}, f) (Refs. 2 and 52). Our measurements indicate that it persists at least for compound nucleus excitation energies up to about 15 MeV. Apart from the $Z=50$ and more symmetric mass region a charge polarization resulting in a higher charge-to-mass ratio for the light fragments is present for the photofission of ^{235}U and ^{238}U, as can be seen in Figs. 1 and 2. The average deviation of Z_p from the unchanged charge density value $\langle \Delta Z \rangle = \langle Z_p - Z_{UCD} \rangle$, excluding the $Z=50$ region, turns out to be nearly independent of the average excitation energy of the compound nucleus in our studies: For the photofission of ^{235}U and ^{238}U $\langle \Delta Z \rangle$ values around 0.40 and 0.25 charge units, respectively, are obtained. This value for ^{238}U can be compared with the value 0.05 ± 0.35 obtained by averaging over experiments at different bremsstrahlung end point energies by Gäggeler and von Gunten.[53] A higher charge-to-mass ratio of the light fragments compared to the compound nucleus ratio, except in the $Z=50$ region, is also observed in ^{235}U(n_{th}, f) (Ref. 2), where ΔZ, modulated by the proton odd-even effect, fluctuates between 0.4 and 0.7 charge units.

The dashed line in the 20-MeV sections of Figs. 1 and 2 indicate the results of static scission point
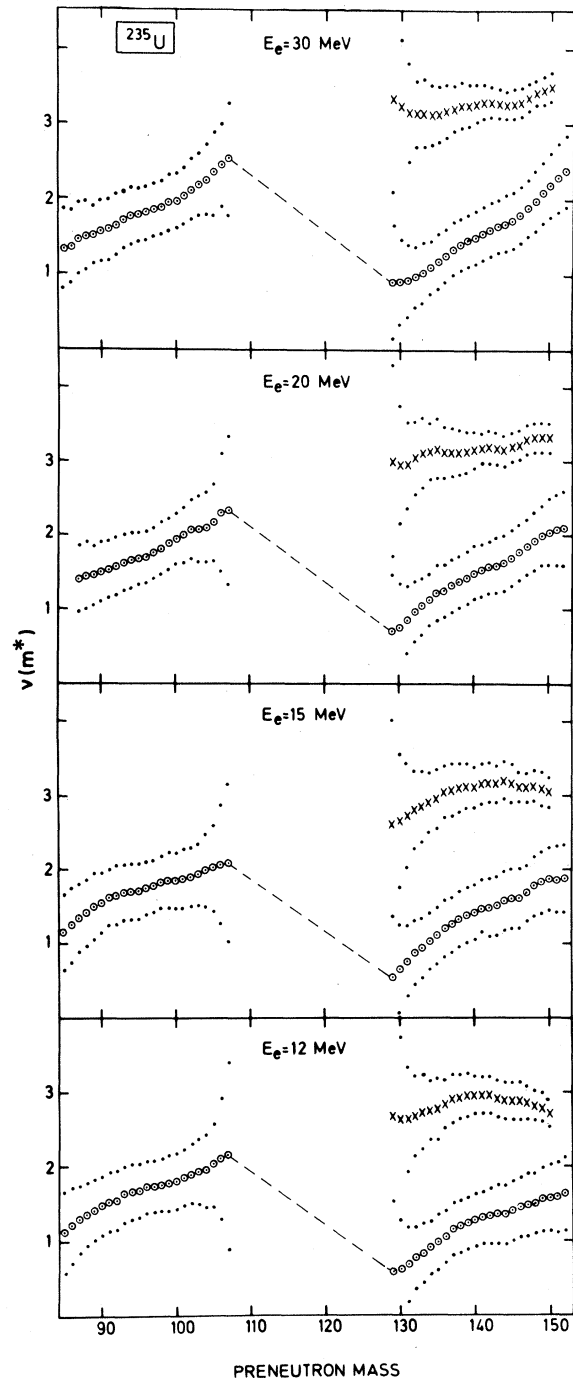
PRENEUTRON MASS

FIG. 3. Neutron emission curves $v(m^*)$ as a function of the preneutron emission mass m^* for the photofission of ^{235}U with 12-, 15-, 20-, and 30-MeV bremsstrahlung. The error bar limits on the calculated $v(m^*)$ values are indicated by the closed points. The crosses represent the total number of neutrons emitted by two complementary fragments as a function of the heavy fragment mass.
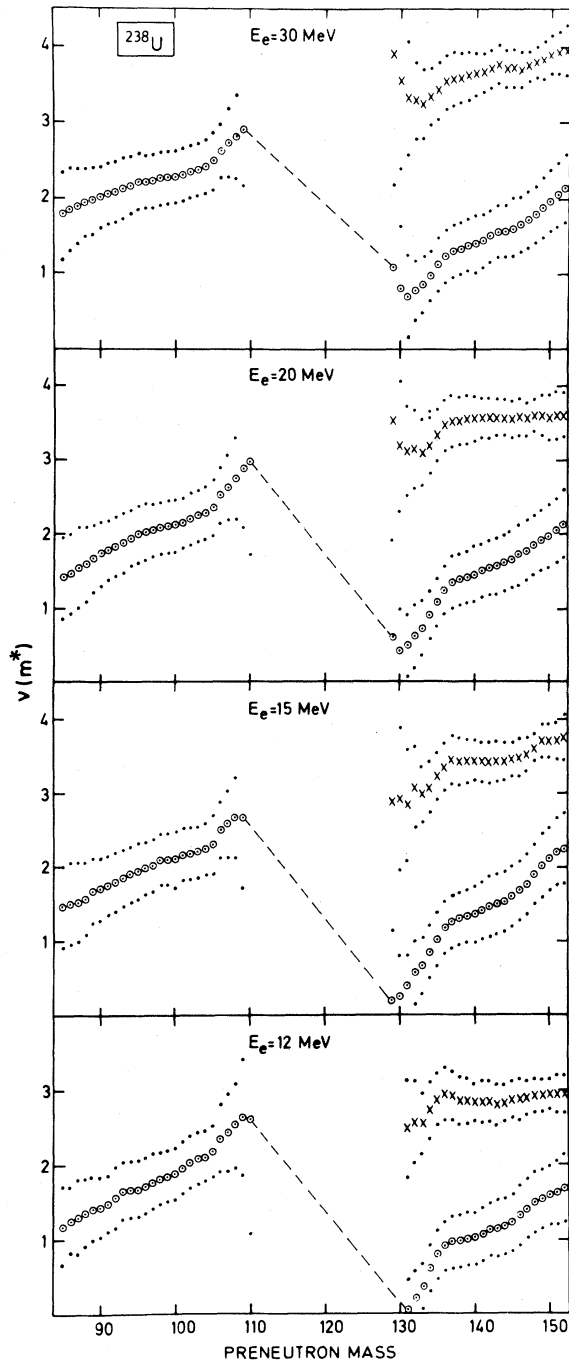
FIG. 4. Neutron emission curves $v(m^*)$ as a function of the preneutron mass m^* for the photofission of ^{238}U with 12-, 15-, 20-, and 30-MeV bremsstrahlung. The symbols have the same meaning as in Fig. 3.

model calculations based on the work of Wilkins *et al.*[11] by Moreau and Heyde.[54] In view of the absence of odd-even effects in the present experiments, a value of 1 MeV was chosen for the intrinsic tem-

perature τ. For the separation distance between the tips of the spheroids d a value of 1.5 fm was used in the calculations (more details will be given in a forthcoming paper). Excluding the mass region around closed shells, the agreement between the calculated and experimentally determined ΔZ values is satisfactory for ^{235}U as well as for ^{238}U. In the case of ^{235}U(n_{th},f) the structures in the behavior of ΔZ, owing to the odd-even effects, are well reproduced by the calculations of Wilkins *et al.*,[11] but the calculated ΔZ values are systematically about 0.2 charge units too low. It was pointed out that this disagreement can be eliminated by the use of an increased value for d in the calculations (Ref. 2). As can be seen in Figs. 1 and 2 the influence of the $Z=50$ shell on the charge distribution, observed in our photofission studies, is not reproduced by the scission point model calculations. This discrepancy in the mass region affected by the $Z=50$ closed shell is also present in ^{235}U(n_{th},f) (Ref. 2). The reason why this model, based on deformed-shell effects in the fragments, fails in predicting this $Z=50$ influence on the charge distribution is not obvious.

The open squares and circles in Figs. 1 and 2 represent the expectation values calculated with the empirical relation of Nethaway[10] for the light and heavy product masses, respectively. In this relation the shift of Z_p for a product mass with respect to the value of the reference system ^{235}U(n_{th},f) is expressed as a linear function of the charge, mass, and excitation energy of the compound nucleus. In our calculations we used the values for the average excitation energy of the ^{235}U and ^{238}U compound nucleus, given in Tables IV and V, respectively. Figures 1 and 2 show that the agreement between the experimentally determined Z_p values and the predictions of Nethaway is very good, except again in the vicinity of the $Z=50$ closed shell, where a serious discrepancy exists. As discussed in a previous paper[13] sudden changes in the behavior of the Z_p function, caused by shell effects, cannot be taken into account in the formula of Nethaway, so that reasonable estimates for Z_p in the $Z=50$ mass region using this method cannot be expected. We can conclude that the relation of Nethaway, which was deduced from neutron induced and spontaneous fission data, is also very valuable for the calculation of the Z_p behavior in photofission except in the closed shell mass regions.

IV. CONCLUSIONS

In the performed photofission experiments the width of the charge distribution is found to be al-

most independent of the average excitation energy of the compound nucleus in the energy range 9.7 − 14.7 MeV. For ^{235}U as well as for ^{238}U, values for the width parameter c very close to those reported in the literature for low-energy fissioning systems are obtained. The observed independence of the width of the charge distribution can be understood in a thermodynamic equilibrium model, if the quantum mechanical zero-point motion dominates over the temperature effects.

In all the studied photofission cases, the behavior of the most probable charge Z_p as a function of the fragment mass shows the influence of the $Z=50$ shell on the charge distribution as also observed in ^{235}U(n_{th},f). Furthermore, a comparison of the experimentally determined Z_p values with the unchanged charge density values indicates a charge polarization in the fissioning nucleus resulting in a higher charge-to-mass ratio of the light fragments, independent of the bremsstrahlung end point energy.

The Z_p behavior, deduced from our photofission measurements on ^{235}U and ^{238}U, is reproduced well by calculations following the scission-point model of Wilkins et al.[11] and by the predictions using the empirical relation of Nethaway[10] except in the $Z=50$ mass region.

ACKNOWLEDGMENTS

[1]G. Mariolopoulos, Ch. Hamelin, J. Blachot, J. P. Bocquet, R. Brissot, J. Crançon, H. Nifenecker, and Ch. Ristori, Nucl. Phys. A361, 213 (1981).

[2]W. Lang, H. G. Clerc, H. Wohlfarth, H. Schrader, and K. H. Schmidt, Nucl. Phys. A345, 34 (1980).

[3]H. O. Denschlag, H. Braun, W. Fankel, G. Fischbach, H. Meveler, G. Paffrath, W. Pörsch, M. Weis, H. Schrader, G. Siegert, J. Blachot, Z. B. Alfassi, H. N. Erten, T. Izak-Biran, T. Tammai, A. C. Wahl, and K. Wolfsberg, in Proceedings of the Fourth International Atomic Energy Agency Symposium on Physics and Chemistry of Fission, Jülich, 1979 (IAEA, Vienna, 1980), Vol. II, p. 153.

[4]B. D. Pate, J. S. Foster, and L. Yaffe, Can. J. Chem. 36, 1691 (1958).

[5]L. Yaffe, in Proceedings of the Second International Atomic Energy Agency Symposium on Physics and Chemistry of Fission, Vienna, 1969 (IAEA, Vienna, 1969), p. 701.

[6]J. A. McHugh and M. C. Michel, Phys. Rev. 172, 1160 (1968).

[7]A. C. Wahl, A. E. Norris, R. A. Rouse, and J. C. Williams, in Proceedings of the Second International Atomic Energy Agency Symposium on Physics and Chemistry of Fission, Vienna, 1969 (IAEA, Vienna, 1969), p. 813.

[8]J. P. Bocquet, R. Brissot, J. Crançon, and A. Moussa, Nucl. Phys. A189, 556 (1972).

[9]D. De Frenne, H. Thierens, E. Jacobs, P. De Gelder, A. De Clercq, P. D'hondt, and A. J. Deruytter, Phys. Rev. C 21, 629 (1980).

[10]D. R. Nethaway, University of California Radiation Laboratory Report No. UCRL-51538, 1974 (unpublished).

[11]B. D. Wilkins, E. P. Steinberg, and R. R. Chasman, Phys. Rev. C 14, 1832 (1976).

[12]E. Jacobs, H. Thierens, D. De Frenne, A. De Clercq, P. D'hondt, P. De Gelder, and A. J. Deruytter, Phys. Rev. C 19, 422 (1979).

[13]E. Jacobs, H. Thierens, D. De Frenne, A. De Clercq, P. D'hondt, P. De Gelder, and A. J. Deruytter, Phys. Rev. C 21, 237 (1980).

[14]D. F. Morris and D. Scargill, Anal. Chim. Acta 14, 57 (1956).

[15]B. J. Dropesky and C. J. Orth, J. Inorg. Nucl. Chem. 24, 1301 (1962).

[16]D. E. Troutner, M. Eichor, and C. Pace, Phys. Rev. C 1, 1044 (1970).

[17]J. G. Cuninghame, J. A. B. Goodall, G. P. Kitt, C. B. Welster, and H. H. Willis, Atomic Energy Research Establishment Report No. AERE-R5587, 1967 (unpublished).

[18]A. De Clercq, H. Thierens, D. De Frenne, P. De Gelder, P. D'hondt, E. Jacobs, and A. J. Deruytter, Nucl. Instrum. Methods 173, 531 (1980).

[19]U. Reus, W. Westmeier, and I. Warnecke, Gesellschaft für Schwerionenforschung Report GSI-79-2, 1979 (unpublished).

[20]J. Blachot and C. Fiche, At. Data Nucl. Data Tables 20, 241 (1977).

[21]H. Thierens, D. De Frenne, E. Jacobs, A. De Clercq, P. D'hondt, and A. J. Deruytter, Nucl. Instrum. Methods 134, 299 (1976).

[22]H. Thierens, D. De Frenne, E. Jacobs, A. De Clercq, P. D'hondt, and A. J. Deruytter, Phys. Rev. C 14, 1058 (1976).

[23]D. C. Kocher, Nucl. Data Sheets 16, 445 (1975).

[24]L. R. Medsker, Nucl. Data Sheets 8, 599 (1972).

[25]T. A. Khan, W. D. Lauppe, K. Sistemich, H. Lawin, G. Sadler, and H. A. Selle, Z. Phys. A 283, 105 (1977).

[26]F. E. Bertrand, Nucl. Data Sheets 10, 91 (1973).

[27]H. Huck, M. L. Perez, and J. J. Rossi, Phys. Rev. C 26, 621 (1982).

[28]B. Fogelberg, K. Heyde, and J. Sau, Nucl. Phys. A352, 157 (1981).

[29]H. R. Hiddleston and C. P. Browne, Nucl. Data Sheets 13, 133 (1974).

[30]J. K. Tuli, Nucl. Data Sheets 23, 529 (1978).

[31]H. O. Denschlag, private communication.

[32]W. Westmeier, private communication.

[33]J. B. Cumming, National Academy of Sciences, Nuclear Science Series Report NAS NS-3107, 1962 (unpublished).

[34]P. O. Strom, G. Grant, and A. C. Pappas, Can. J. Chem. 43, 2493 (1965).

[35]M. Diksic and L. Yaffe, Can. J. Chem. 53, 3116 (1975).

[36]A. Kerek, G. B. Holm, S. Borg, and L. E. De Geer, Nucl. Phys. A195, 177 (1972).

[37]H. Huck, M. L. Perez, J. J. Rossi, and H. M. Sofia, Phys. Rev. C 24, 2227 (1981).

[38]L. I. Schiff, Phys. Rev. 83, 252 (1951).

[39]J. T. Caldwell, E. J. Dowdy, B. L. Berman, R. A. Alvarez, and P. Meyer, Phys. Rev. C 21, 1215 (1980).

[40]A. C. Shotter, D. Branford, J. C. McGeorge, and J. M. Reid, Nucl. Phys. A210, 55 (1977).

[41]S. Amiel and H. Feldstein, in *Proceedings of the Third International Atomic Energy Agency Symposium on Physics and Chemistry of Fission, Rochester, 1973* (IAEA, Vienna, 1974), Vol. II, p. 65.

[42]J. C. Hardy, L. C. Carraz, B. Jonson, and P. G. Hansen, Phys. Lett. 71B, 307 (1977).

[43]H. G. Clerc, W. Lang, H. Wohlfarth, H. Schrader, and K. H. Schmidt, in *Proceedings of the Fourth International Atomic Energy Agency Symposium on Physics and Chemistry of Fission, Jülich, 1979* (IAEA, Vienna, 1980), Vol. II, p. 65.

[44]H. A. Nifenecker, J. Blachot, J. P. Bocquet, R. Brissot, J. Crançon, C. Hamelin, G. Mariolopoulos, and C. Ristori, in *Proceedings of the Fourth International Atomic Energy Agency Symposium on Physics and Chemistry of Fission, Jülich, 1979* (IAEA, Vienna, 1980), Vol. II, p. 35.

[45]R. Vandenbosch and J. R. Huizenga, *Nuclear Fission* (Academic, New York, 1973).

[46]E. Jacobs, A. De Clercq, H. Thierens, D. De Frenne, P. D'hondt, P. De Gelder, and A. J. Deruytter, Phys. Rev. C 20, 2249 (1979).

[47]E. Jacobs, A. De Clercq, H. Thierens, D. De Frenne, P. D'hondt, P. De Gelder, and A. J. Deruytter, Phys. Rev. C 24, 1795 (1981).

[48]E. Jacobs, H. Thierens, A. De Clercq, D. De Frenne, P. D'hondt, and A. J. Deruytter, Phys. Rev. C 14, 1874 (1976).

[49]J. Terrell, Phys. Rev. 127, 880 (1962).

[50]E. E. Maslin, A. L. Rodgers, and W. G. F. Core, Phys. Rev. 164, 1520 (1967).

[51]J. W. Boldeman, A. R. L. Musgrove, and R. L. Walsh, Aust. J. Phys. 24, 821 (1971).

[52]J. Kratz and G. Herrmann, in *Proceedings of the Third International Atomic Energy Agency Symposium on Physics and Chemistry of Fission, Rochester, 1973* (IAEA, Vienna, 1974), Vol. II, p. 95.

[53]H. Gäggeler and H. R. von Gunten, J. Inorg. Nucl. Chem. 40, 1859 (1978).

[54]J. Moreau and K. Heyde, private communication.